Evidence for the Extended Helical Nature of Polysaccharide Epitopes. The 2.8 Å Resolution Structure and Thermodynamics of Ligand Binding of an Antigen Binding Fragment Specific for α-(2→8)-Polysialic Acid‡

S. V. Evans,*,∞,▽ B. W. Sigurskjold,▽,§ H. J. Jennings,*,▽ J.-R. Brisson,▽ R. To,▽ W. C. Tse,▽ E. Altman,▽ M. Frosch,|| C. Weisgerber,▽ H. D. Kratzin,△ S. Klebert,△ M. Vaesen,△ D. Bitter-Suermann,|| D. R. Rose,▽,⊥ N. M. Young,▽ and D. R. Bundle▽,#

Institute for Biological Sciences, National Research Council of Canada, Ottawa, Canada K1A 0R6, Max-Planck Institut für Experimentelle Medizin, Abteilung Immunchemie, 37075 Göttingen, Germany, and Medizinische Hochschule Hannover, Institut für Medizinische Mikrobiologie, 30625 Hannover, Germany

Received May 23, 1994; Revised Manuscript Received November 9, 1994⊗

ABSTRACT: The antigen binding fragment from an IgG_{2a} κ murine monoclonal antibody with specificity for α-(2→8)-linked sialic acid polymers has been prepared and crystallized in the absence of hapten. Crystals were grown by vapor diffusion equilibrium with 16−18% polyethylene glycol 4000 solutions. The structure was solved by molecular replacement methods and refined to a conventional *R* factor of 0.164 for data to 2.8 Å. The binding site is observed to display a shape and distribution of charges that is complementary to that of the predicted conformation of the oligosaccharide epitope. A thermodynamic description of ligand binding has been compiled for oligosaccharides ranging in length from 9 to 41 residues, and the data for the largest ligand has been used in a novel way to estimate the size of the antigen binding site. A model of antigen binding is presented that satisfies this thermodynamic data, as well as a previously reported requirement of conformational specificity of the oligosaccharide. X-ray crystallographic and thermodynamic evidence are consistent with a binding site that accommodates at least eight sialic acid residues.

The capsular polysaccharides of group B meningococci and *Escherichia coli* capsular type K1, which both cause human meningitis, consist of a homopolymer of α-(2→8)-linked sialic acid (*N*-acetylneuraminic acid; Jennings *et al.*, 1984). The polymer is known to be poorly immunogenic (Wyle *et al.*, 1972; Jennings & Lugowski, 1981). That this poor immunogenicity is due to molecular mimicry is supported by the identification of structurally identical α-(2→8)-linked sialooligosaccharides in human and animal fetal tissue (Finne *et al.*, 1983). Chains of α-(2→8)-linked sialic acid are developmental antigens (Rutishauser & Jessel, 1988a), are carried by glycoproteins involved in neural cell adhesion (Rutishauser *et al.*, 1988b; Phillips *et al.*, 1990; Brandley *et al.*, 1990; Corral *et al.*, 1990; Berg *et al.*, 1991), and have also been identified in other tissues including human tumors (Troy, 1992). Despite its poor antigenicity, antibodies to α-(2→8)-polysialic acid can be produced in special circumstances. One such monoclonal antibody (IgG_{2a}, designated mAb735) has been characterized (Frosch *et al.*, 1985), and its heavy and light chains have been sequenced (Vaesen *et al.*, 1991; Klebert *et al.*, 1993).

This antibody, its Fab,[1] and other α-(2→8)-polysialic acid specific antibodies all require an unusually long segment of hapten for binding, and the affinity appears to increase with increasing chain length (Jennings *et al.*, 1984, 1985; Finne & Mäkelä, 1985; Kabat *et al.*, 1988; Häyrinen *et al.*, 1989). It has been proposed that antibodies recognize a specific helical conformation of this polysaccharide and a minimum of 10 residues is required to form a helical epitope. The validity of this proposition was further strengthened by the identification of a common length-dependent epitope responsible for the cross-reaction of α-(2→8)-polysialic acid and poly(A) with a human monoclonal macroglobulin (IgM^{NOV}; Kabat *et al.*, 1988) and the known propensity of poly(A) to form helices of $n = 8-10$ (Yanthindra & Sundaralingam, 1976). This conformational dependence on chain length has been confirmed by NMR (Michon *et al.*, 1987), and similar chain length-dependent conformational epitopes have been described for other antigenic capsular polysaccharides (Wessels *et al.*, 1987; Wessels & Kasper, 1989). By means of potential energy calculations and NMR, it was shown that, although mostly random coil in nature, α-(2→8)-polysialic acid can adopt extended helical conformations where $n \approx 9$ (Brisson *et al.*, 1992), the stability

‡ Coordinates have been deposited with the Protein Data Bank at Brookhaven National Laboratories, code 1PLG.

* Corresponding authors.

∞ Present address: Department of Biochemistry, University of Ottawa, 451 Smyth, Ottawa, Canada K1H 8M5.

▽ National Research Council of Canada.

§ Present address: Department of Chemistry, Carlsberg Laboratory, Valby, Copenhagen DK-2500, Denmark.

△ Max-Planck Institut für Experimentelle Medizin.

|| Medizinische Hochschule Hannover.

⊥ Present address: Ontario Cancer Institute and Department of Medical Biophysics, University of Toronto, 500 Sherbourne St., Toronto, Ontario, Canada M4X 1K9.

Present address: University of Alberta, Department of Chemistry, Edmonton, Alberta, Canada T6G 2G2.

⊗ Abstract published in *Advance ACS Abstracts,* February 15, 1995.

[1] Abbreviations: ELISA, enzyme-linked immunosorbent assay; Fab, antigen binding fragment; PEG, polyethylene glycol; L1, L2, L3, H1, H2, and H3, the six hypervariable loops as defined by Kabat *et al.* (1991); HEPES, *N*-(2-hydroxyethyl)piperazine-*N*′-2-ethanesulfonic acid; SDS−PAGE, sodium dodecyl sulfate−polyacrylamide gel electrophoresis.

0006-2960/95/0434-6737$09.00/0 Published 1995 by the American Chemical Society

of which are dependent on its carboxylate groups (Baumann *et al.*, 1993). It has also been shown that mAb735 displays a fairly high degree of specificity for the *N*-acetylneuraminic acid polymer, as there is only a small cross-reactivity (≈5%) observed with the *N*-propyl analogue (Jennings *et al.*, unpublished results).

The determination of the three-dimensional structure of the antigen binding fragment and a thermodynamic description of the hapten binding of such a system are necessary steps in extending our understanding of the interactions between antibodies and specific conformations of antigenic polysaccharides. We now report the preparation, thermodynamic characterization, crystallization, molecular replacement solution, and 2.8 Å resolution structure of a Fab from the murine monoclonal antibody mAb735 specific for α-(2→8)-linked polysialic acid. We also present the results of modeling studies on the nature of the antibody−antigen complex carried out using the structure of the binding site reported herein and the structure of the antigen previously reported from NMR experiments (Brisson *et al.*, 1992).

EXPERIMENTAL PROCEDURES

Preparation of Fab. The Fab was prepared by digesting 30.4 mg of mAb735 (IgG_{2a}) in 15 mL of 10 mM Tris·HCl containing 50 mM dithiothreitol (pH 8.0) with 152 μg of papain (IgG:papain = 200:1) for 5 h at room temperature. The solution was dialyzed at 4 °C against three changes of 10 mM Tris·HCl (pH 8.0) and applied to a DE52 ion exchange column. The Fab fragment was eluted with the same buffer. SDS−PAGE of the purified Fab under reducing conditions showed two bands of apparent molecular weight 30 and 26 kDa, corresponding to the Fd and L chains of the Fab, and isoelectric focusing showed a single band at p*I* 8.4.

Preparation of Oligomers of Sialic Acid. Oligomers of sialic acid were obtained by partial acid hydrolysis of the sodium salt of colominic acid purchased from Nacalai Tesque, Inc. (Kyoto, Japan); 100 mg of colominic acid was dissolved in 3 mL of water, the pH brought down to 2.0, and the sample heated to 80 °C for 1 h. After cooling, the pH was adjusted to 7.0, and crude fractions of varying molecular weight with chain lengths ranging from 9 to 15 were obtained from BioGel P-10, 200−400 mesh (BioRad Laboratories) chromatography eluted with 30 mM ammonium bicarbonate buffer, pH 8.0. The fractions were dialyzed against water and lyophilized. Further purification was carried out by preparative exchange chromatography (Dionex anion) using a Carbo-Pac PA1 (9 × 250 mm) column with pulsed amperometric detection. The eluant consisted of 0.15 M sodium hydroxide with a gradient from 50 mM to 1 M sodium acetate (followed by post column addition of 0.5 M sodium hydroxide). After passage through the detector, the eluant fractions were immediately adjusted to pH 7.0 with acetic acid. A homogeneous preparation of colominic acid corresponding to an approximately 12 kDa polymer (equivalent to approximately 41 residues) was obtained as the highest molecular weight fraction from Sephadex G-100 chromatography of the sodium salt of colominic acid using 10 mM sodium phosphate, 0.15 M sodium chloride, pH 7.2.

Microcalorimetry. The thermodynamic parameters for the binding of the α-(2→8)-linked sialic acid polymer by the mAb735 Fab were obtained by titration calorimetry using an OMEGA titration microcalorimeter from MicroCal Inc., (Northampton, MA) (Wiseman *et al.*, 1989). A solution of 76 μM Fab in 10 μM sodium potassium phosphate buffer containing 0.15 M sodium chloride, pH 7.4, was titrated at 25 °C with ligand in the same buffer. Twenty injections of 5 μL from a 100 μL syringe stirring at 400 rpm were carried out from a solution of 13.35 mg/mL ligand. The thermodynamics of the binding of oligomers to mAb735 IgG was determined in the same way. Data analysis of the binding isotherms was carried out as described previously (Sigurskjold *et al.*, 1991).

Crystallization and X-ray Diffraction Analysis. Crystals of mAb735 were obtained by the hanging drop method. The reservoir solution was composed of 16−18% PEG-4000, 0.1 M HEPES at pH 7.5, 0.1 M $(NH_4)_2SO_4$, and 0.01 M NaN_3. The drops were made by mixing 6.0 μL of 6.7 mg/mL Fab with 6.0 μL of reservoir solution on the coverslip and seeded 1 day later with microcrystals grown previously. Crystals appeared after 1 week and grew to an average size of 0.3 × 0.3 × 0.4 mm^3. Crystals of mAb735 are orthorhombic, with a = 79.14 Å, b = 91.21 Å, and c = 141.4 Å. Systematic absences showed the space group to be either $I222$ or $I2_12_12_1$, with one molecule per asymmetric unit.

X-ray diffraction data from a single crystal were collected on a San Diego multiwire system two-detector setup mounted on a Rigaku RU-200 rotating anode X-ray generator operated at 40 kV and 120 mA. The detectors were positioned at θ values of −12.0° and 30.0°, and the diffraction sphere was sampled in seven sweeps. A total of 87625 measurements were made of 10 590 unique reflections, out of a total of 10 611 possible reflections, yielding a data set 99.8% complete to 2.8 Å resolution. No explicit corrections for absorption or decay were applied.

Molecular Replacement Solution. The structure was solved in space group $I222$ *via* molecular replacement methods. Solution proceeded in two stages, using the anti-*Brucella abortus* YsT9.1 Fab structure (Rose *et al.*, 1993) as a model. First, the orientation and position of the constant region were determined using the MERLOT package (Fitzgerald, 1988). Many combinations of resolution range and σ cutoff were tried, with the cleanest results obtained using data in the range 6.0−4.0 Å resolution with $I \geq 3\sigma(I)$.

The positioning of the variable region was less straightforward, as no combination of data range and σ cutoff using MERLOT led to a solution. The correct position of this fragment was located *via* a packing serach utilizing the now correctly positioned constant region, by allowing the variable region to rotate about the Fab 'hinge' residues in 2° intervals, while monitoring all intra- and intermolecular contacts. This procedure defined an allowed section of approximately 15° of arc in which the variable region could be accommodated by the crystal packing. However, a six-dimensional fine grid search about the allowed section using the entire variable region of the YsT9.1 Fab model did not yield a match to the observed diffraction pattern. The final molecular replacement solution required the separate positioning of the heavy and light chains of the variable region of the Fab, using the program BRUTE (Fujinaga and Read, 1987), with the entire constant region input as a stationary atoms set.

All refinements were carried out with the program XPLOR (Brünger *et al.*, 1988) using data in the resolution range 6.0−2.8 Å with an $F \geq 3\sigma(F)$ cutoff and using the sequence for

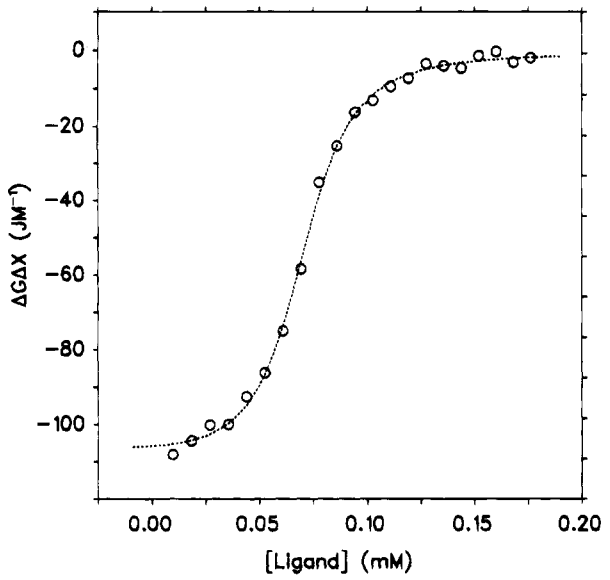

FIGURE 1: Isotherm for the binding of the Fab to the 12 kDa α-(2→8)-linked sialic acid oligomer. The dotted line shows the calculated fit (Sigurskjold *et al.*, 1991) assuming that two Fabs bind each 41-mer oligosaccharide.

the YsT9.1 model. Rigid body refinement of the molecular replacement solution of the mAb735 began with just the variable and constant regions defined as rigid bodies and then with each of those divided into heavy and light chains. After a total of 50 cycles, the *R* factor dropped to 0.33 from the initial 0.48. Refinement proceeded with several rounds of simulated annealing with an initial temperature of 3500 K. Conventional positional refinement with an overall temperature factor applied further reduced the *R* factor to 0.26 after 50 cycles. After a single round of manual intervention, refinement proceeded again using an overall temperature factor to yield an *R* factor of 0.24 after an additional 50 cycles. To avoid biasing the struture, no water molecules were included in the refinement.

At this point in refinement, the sequences for both the heavy and light chains became known (Vaesen *et al.*, 1991; Klebert *et al.*, 1993) and were imposed on the structure. The final set of refinements included the placement of 41 water molecules and individual atomic temperature factors were allowed to refine. Convergence was reached after a total of 50 cycles to yield a final *R* factor of 0.164 at a resolution of 2.8 Å.

RESULTS AND DISCUSSION

Thermodynamics. Three parameters can be obtained from nonlinear regression analysis of the calorimetric isotherm: the molar enthalpy ($\Delta H°$), the binding constant (K), and the apparent concentration of binding sites (Fab) (Wiseman *et al.*, 1989; Sigurskjold *et al.*, 1991), and from these values, $\Delta G°$ and $\Delta S°$ can be calculated. The isotherm for the binding of the Fab to the 12 kDa α-(2→8)-linked sialic acid polymer consisting of approximately 41 residues is shown in Figure 1. (Unless otherwise stated, all figures were generated with the SETOR program package; Evans, 1993.) This isotherm is a smooth sigmoid curve, *i.e.*, it describes only a single binding constant. This means that if there is more than one epitope on this polysaccharide chain, then the binding of one Fab to the polysaccharide does not significantly facilitate (nor debilitate) the binding of a subsequent Fab. Such cooperativity in binding has been observed, *e.g.* , for the type III group B *Streptococcus* capsular polysaccharide (Wessels *et al.*, 1987). The isotherm was fitted four times assuming that the polymer contained either one, two, three, or four epitopes for binding to the Fab, respectively, and the apparent concentration of Fab was determined in each fit. The regression results are shown in Table 1, and only the value of 73 μM Fab—corresponding to two epitopes on the ligand—is consistent with the known concentration of 76 μM Fab. It is concluded that a polymer of approximately 41 sialic acid residues can accommodate only two Fab molecules. The calorimetric measurements therefore provide an estimate of the extent to which an individual Fab renders adjacent segments of the antigen chain unavailable for binding. In this case, the maximum number of sialic acid residues involved is from 15 to 20, a number that is consistent with a binding site around 10 residues in length. This also demonstrates a novel use of calorimetry to determine the size of a binding epitope. The association is enthalpy driven with a large unfavorable change in entropy. Strong enthalpic interactions combined with unfavorable entropy changes are usually observed for protein—carbohydrate interactions with long sugar chain lengths [Sigurskjold *et al.* (1991) and references therein].

For comparison the thermodynamics of the binding of the whole mAb735 IgG to oligomers from 9 to 15 residues in length are shown in Table 2. The binding of these ligands ($K_A \approx 4 \times 10^4$ M^{-1}) is 1 order of magnitude weaker than for the long chain ($K_A \approx 3 \times 10^5$ M^{-1}). There seems to be little or no chain length dependence for any of the thermodynamic functions in this range of chain lengths, which seems to contrast with previous observations (Jennings *et al.*, 1984, 1985; Finne & Mäkelä, 1985; Kabat *et al.*, 1988; Häyrinen *et al.*, 1989); however, this trend may be concealed by the large standard deviations observed for $-T\Delta S°$. We can observe a relatively strong chain length dependence between binding of the long polymer and the shorter oligomers. The enthalpy of binding for the long polymer is twice that of the shorter ligands. Thus it seems that the Fab is able to take full advantage of the enthalpic interactions for the whole epitope of about 20 residues. The entropy change, on the other hand, has become progressively more unfavorable, $-T\Delta S°$ being 3 times greater for the polymer than for the shorter oligomers and thus compensating for some of the enthalpy gain. This reflects that—as expected—there is a strong entropy penalty in binding longer chains (if $-T\Delta S°$ for the polymer were just twice that of the oligomers, K would be about 10^9 M^{-1}).

X-ray Crystal Structure Analysis. A summary of the deviations between stereochemical parameters derived from the final cycle of refinement with ideal values (Table 3) shows that this structure displays geometry that is in good agreement with literature values and has all non-glycine residues, with the exception of V56 on the light chain, in or near the allowed regions of a Ramachandran plot, Figure 2. Additionally, examination over the course of the polypeptide chain shows that, with a few exceptions distant from the binding site, all main chain and side chain atoms are observed to occupy appropriate electron density. Figure 3 is an electron density map of the heavy chain H1, which illustrates the well-defined density that is typical for residues in the hypervariable loops.

Table 1: Thermodynamics and Determination of Epitope Size of the Binding by mAb735 Fab of a 12 kDa Polymer of α-(2→8)-Linked Sialic Acid (Corresponding to Approximately 41 Residues) Obtained by Titration Microcalorimetry[a]

assumed no. of epitopes	K ($\times 10^{-5}$ M^{-1})	$\Delta G°$ (kJ M^{-1})	$\Delta H°$ (kJ M^{-1})	$-T\Delta S°$ (kJ M^{-1})	apparent conc of Fab (μM)
1	7.3 ± 4.0[b]	-33.8 ± 1.4	-161.6 ± 15.1	127.8 ± 15.8	37 ± 4
2	3.4 ± 2.0	-31.9 ± 1.5	-81.6 ± 8.5	49.8 ± 9.3	73 ± 8
3	2.4 ± 1.4	-31.0 ± 1.4	-54.1 ± 5.3	23.1 ± 6.1	110 ± 13
4	1.7 ± 0.9	-30.1 ± 1.4	-41.0 ± 4.1	10.9 ± 4.9	146 ± 17

[a] The concentration of mAb735 Fab in the experiment was 76 μM. [b] Uncertainties represent three standard deviations.

Table 2: Chain Length Dependence of the Binding of α-(2→8)-Linked Sialic Acid Oligomers to mAb735 IgG Obtained by Titration Microcalorimetry

chain length	K ($\times 10^{-4}$ M^{-1})	$\Delta G°$ (kJ M^{-1})	$\Delta H°$ (kJ M^{-1})	$-T\Delta S°$ (kJ M^{-1})
9	3.9 ± 0.9[a]	-26.2 ± 0.6	-45.4 ± 6.7	19.1 ± 6.8
11	4.8 ± 0.9	-26.7 ± 0.5	-42.6 ± 2.9	15.8 ± 2.9
14	5.9 ± 2.9	-27.2 ± 1.2	-38.7 ± 2.8	11.5 ± 3.1
15	4.4 ± 1.9	-26.5 ± 1.1	-41.6 ± 6.8	15.9 ± 7.3
average	4.4 ± 0.9	-26.6 ± 0.5	-41.0 ± 2.6	14.4 ± 2.7

[a] Uncertainties represent three standard deviations.

Table 3: Stereochemistry of the Fab from mAb735 after Refinement to 2.8 Å Resolution

stereochemical refinement parameter	rms deviation from ideal values	refinement restraint weighting parameter
bond distances (Å)	0.014	0.030
angle distances (Å)	0.052	0.040
planar 1−4 distances (Å)	0.065	0.060
planes (Å)	0.022	0.030
chiral volumes (Å^3)	0.125	0.125
ω dihedral angles (deg)	3.5	15.0
single dihedral contacts (Å)	0.232	0.250
multiple dihedral contacts (Å)	0.201	0.250

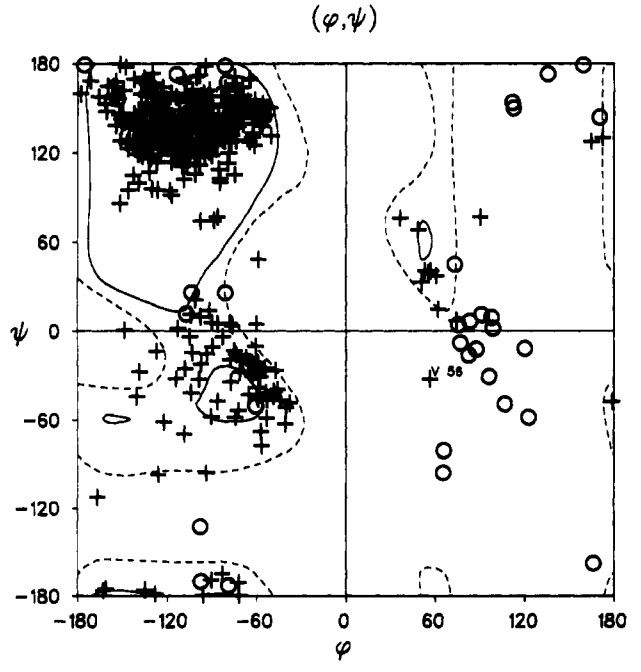

FIGURE 2: Plot of main chain dihedral angles (Ramakrishnan & Ramachandran, 1965) of all non-glycine residues of mAb735.

The framework regions of the molecule adopt conformations similar to those reported for other Fabs and display the usual immunoglobulin fold with an elbow angle between the pseudo-2-fold axes of the variable and constant domain dimers equal to 166°. The molecules are packed in the usual head-to-tail fashion observed for most Fabs, with the long axis of the molecule nearly coincident with the unit cell c-axis. Seven of the 15 observed intermolecular contacts are between residues in the hypervariable regions and the C domain dimers of adjacent molecules, mostly involving the L1 and H1 loops.

As the shape and charge distribution of the oligosaccharide are of paramount importance in describing its antigenic properties, the binding surface of the Fab is also best described in that manner. The antigen binding surface is bimodal in that it undergoes a striking reversal in shape and charge distribution along the interface between the heavy and light chains. The left side of the site (as in Figure 4) is where L3, H2, and the 'tip' of H3 are observed to form a convex surface which displays three positively charged lysine residues, Lys H59, Lys H65, and Lys H101. The right side of the site finds L2 and the bulk of H3 meeting to form a groove which has a relatively uncharged surface except for the negatively charged Asp H105 residue at the bottom of the groove, with positively charged Arg H98 just above it on the side. Loops L1 and H1 display no charged residues except Asp H31, which is well away from the observed groove.

Modeling the Hapten into the Binding Site. X-ray crystallographic studies of complexes of Fabs with oligosaccharides have shown that the specificity of the binding site on the Fabs usually encompasses one to four sugar residues (Cygler *et al.* 1991; Oomen *et al.*, 1991; Vyas *et al.*, 1993); however, there are several reasons to suppose that the binding site on mAb735 is much larger. Firstly, binding studies have demonstrated that a critical chain length of 10 α-(2→8)-linked sialic acid residues is required in order for the hapten to bind to mAb735 (Häyrinen *et al.*, 1989), and this has been confirmed in our thermodynamic analysis. Secondly, NMR studies in conjunction with potential energy calculations (Brisson *et al.*, 1992) are consistent with the presence of an extended helical epitope in α-(2→8)-polysialic acid. Thirdly, from examples where binding studies have been reported (Jennings *et al.*, 1985; Finne & Mäkelä, 1985; Kabat *et al.*, 1988; Häyrinen *et al.*, 1989), all antibodies specific for α-(2→8)-polysialic acid reported to date are based on an extended helical epitope. None have been detected with a specificity for shorter α-(2→8)-sialooligosaccharides. Thus, any model of hapten bound in the binding site of mAb735 must reflect this helical nature of the antigenic form of the hapten and allow contact between antibody and antigen along a span that is of the order of 10 residues in length. Finally, the model must explain the specificity that mAb735 shows for the *N*-acetyl- vs *N*-propylneuraminic acid. Although the ^{1}H NMR analysis provides overwhelming evidence for the requirement of a helical conformation for the antigen, the

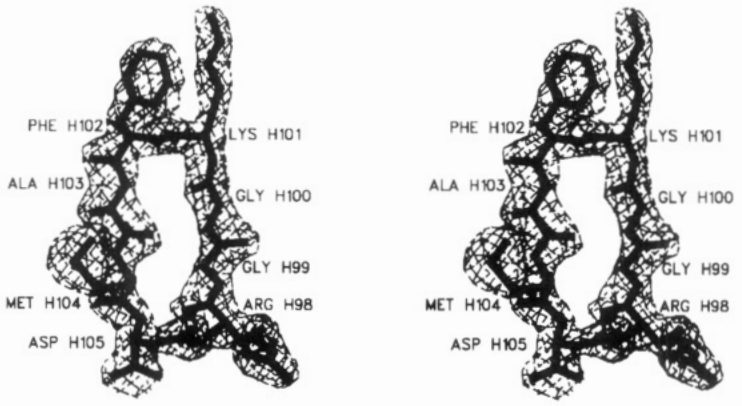

FIGURE 3: Stereoview of the tip of the H3 loop (thick lines) and surrounding residues, showing the corresponding observed electron density (thin lines) plotted at a 1.5σ level. With few exceptions, all residues in the protein display excellent agreement with observed electron density.

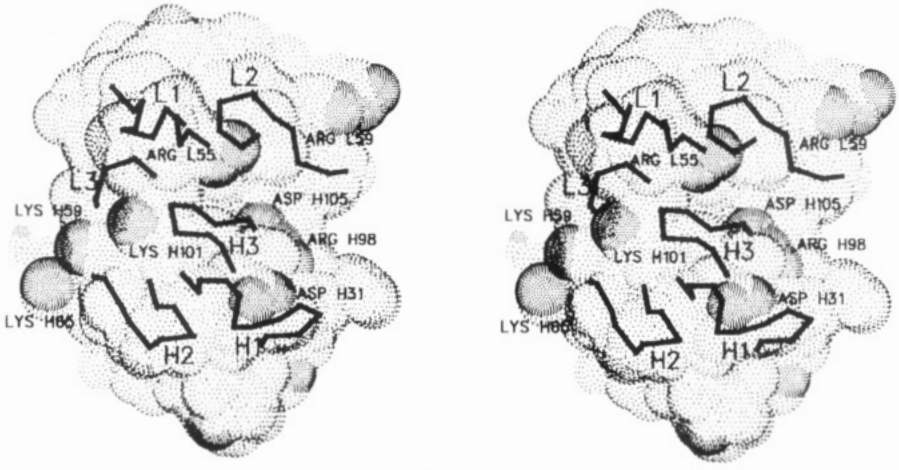

FIGURE 4: Stereoview of the antigen binding surface (Connolly, 1981) of mAb735 looking down the pseudo-2-fold axis. Those portions of the surface due to charged atoms are shown with denser dot distribution and have their parent residues labeled.

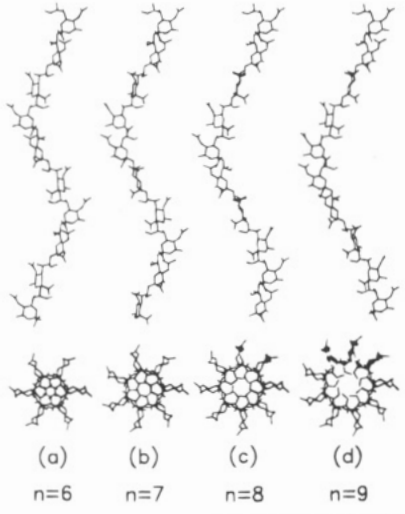

FIGURE 5: Side and top views with respect to the helix axis for helical models of α-(2→8)-linked sialic acid 10-mers constructed to fit ^{1}H NMR solution data (Brisson *et al.*, 1992). Although the pitch of the helix that can be accommodated from the NMR data can vary significantly, all helix models require the negatively charged carboxylic acid groups to face the interior of the helix while the *N*-acetyl groups face the exterior of the helix. The index n shows the number of residues per turn for each helix.

exact pitch of the helix that can be generated to fit this data can vary significantly, Figure 5.

Helices are defined in terms of a set of helical parameters (n,h) with n being the number of residues per turn and h being the translation along the helix axis of corresponding residues. The pitch is defined as $n \times h$. Helices were generated as described before (Brisson *et al.*, 1992). The rise per residue, h, for the $n = 6$ helix was 6.0 Å, and 5.8 Å for the $n = 9$ helix. Extended helices of nearly identical energy can be generated for $n = 6-11$ by a slight change (30°) in only one of the four dihedral angles linking two residues (Brisson *et al.*, 1992). For the $n = 6$ and $n = 9$ helix, this dihedral angle differs by only 20°. This demonstrates that the pitch of these extended helices can vary greatly by minimal rotation about only one bond and with very little change in energy.

All of these helical models of polysialic acid have several important features in common. Most significantly, in each model the negatively charged carboxylic acid groups face the interior of the helix with a repeat distance of 5−8 Å while the *N*-acetyl groups face the exterior of the helix. This means that for any of the models, over one turn of the helix, one end of the oligomer would present the negatively charged carboxylic acid groups to the binding site on the antibody while the midpoint of the oligomer would present the relatively uncharged but protruding *N*-acetyl groups. This reversal of environment from one end of the epitope to the other is the mirror to that described above for the Fab binding site, where one extreme of the binding site presents a series of positively charged lysine groups with the correct spacing to form salt bridges with the carboxylic acid groups on the antigen, while the other extreme of the binding site presents

Table 4: Successive Rotation of Sialic Acid Residues in the Model of Bound Hapten

sialic acid residues	rotation (deg)
2–3	66.5
3–4	58.0
4–5	74.5
5–6	50.3
6–7	72.3
7–8	68.2
8–9	52.6

Table 5: Number and Type of Hydrogen Bonds Found on Oligosaccharide Residues in the Model

sialic acid residue	total	to COO^-	to *N*-acetyl
2	3	0	3
3	7	0	2
4	5	0	3
5	4	2	1
6	4	1[a]	0
7	2	1	0
8	2	1[a]	1
9	2	1[a]	0

[a] Charged residue interaction.

a groove which can accommodate and recognize the *N*-acetyl groups.

The observation of shape and charge complementarity between antibody and antigen strongly suggests a model for mAb735–polysialic acid binding, and unlike the helix models derived from the NMR data, the binding site on the Fab has very definite dimensions and can only accommodate a narrow range of helix pitch. In order for the hapten to form both the salt bridges and be properly oriented to project the *N*-acetyl groups into the observed groove on the surface of the Fab, the oligosaccharide helix must make approximately $^1/_2$ of a turn within 17 Å. This corresponds to helix a of Figure 5, with $n = 6$ residues per turn and a pitch of $n \times h = 36$ Å.

The approach taken for modeling the complex was conservative. No main chain atoms of the protein were moved. Side chain conformations for both the protein and the oligosaccharide were allowed to vary between sterically favored rotamers. In order to best compare the fit between oligosaccharide model and Fab, the basic helical shape of the search model was preserved, and Table 4 shows that the angle of rotation between each successive pair of sugar rings is close to the 60° expected for an $n = 6$ helix. However, small changes in the dihedral angles of the linking regions of the oligosaccharide were required to bring suitable hydrogen-bonding partners into proximity. The NMR data will accommodate a range of pitch for the oligosacchride links, and although the models that are presented in Figure 5 contain links of identical pitch, any model can contain links of different pitch. Two water molecules that had been located in the binding site during the refinement procedure were moved less than 1.0 Å such that the original hydrogen-bonding partner was maintained. A third water molecule, Wat-21, which was in the second hydration shell, had to be removed to make way for the oligosaccharide.

The initial fit of the 10-mer helix in Figure 5a is shown in Figure 6. The three predicted salt bridges with the lysine residues are easily formed with small changes in the dihedral angles of the linking regions of the oligomer, and the turn of the helix is adequate to bring an appropriate *N*-acetyl group as well as much of its parent sugar residue into the groove observed on the face of the Fab. The high degree of complementarity of the initial fit of the helix to the binding surface of the Fab is evident, as each one of eight consecutive residues of the oligosaccharide makes significant overall contact with the protein, forming at least two hydrogen bonds, Table 5 and Figure 7. Table 5 also reflects the helical nature of the antigen, where the first residues in the hapten are bound chiefly through the *N*-acetyl groups, while the latter residues form salt bridges to the carboxylate anions.

With the exception of L1, each of the hypervariable loops can make at least one hydrogen bond directly with the modeled hapten; however, residues on L1 can serve to stabilize the position of a water molecule in a position to form a strong bridge to the hapten, Figure 7. No significant contact is made between the framework residues of the Fab and the oligosaccharide model. Table 5 and Figure 7 both show that the model of the antigenic form of the oligosaccharide can make as many as 30 hydrogen bonds with the Fab, with a $\Delta H°$ of about -41 kJ M^{-1}. This compares well with the crystal structure and thermodynamics (Bundle *et al.*, 1994) of the *Salmonella O*-polysaccharide antigen Fab complex (Cygler *et al.*, 1991), which shows 12 hydrogen bonds with a $\Delta H°$ of about -20 kJ M^{-1}.

FIGURE 6: Stereoview of the fit of the helical model of α-(2→8)-linked sialic acid to the binding surface of Fab mAb735. The Fab is viewed approximately down its pseudo-2-fold axis, with the light chain positioned above and the heavy chain below the hapten. The left side of the diagram shows the salt bridges formed between three surface lysine groups and the corresponding carboxylic acid groups on the hapten. The right side shows the contact of the *N*-acetyl groups of the hapten with surface features on the Fab.

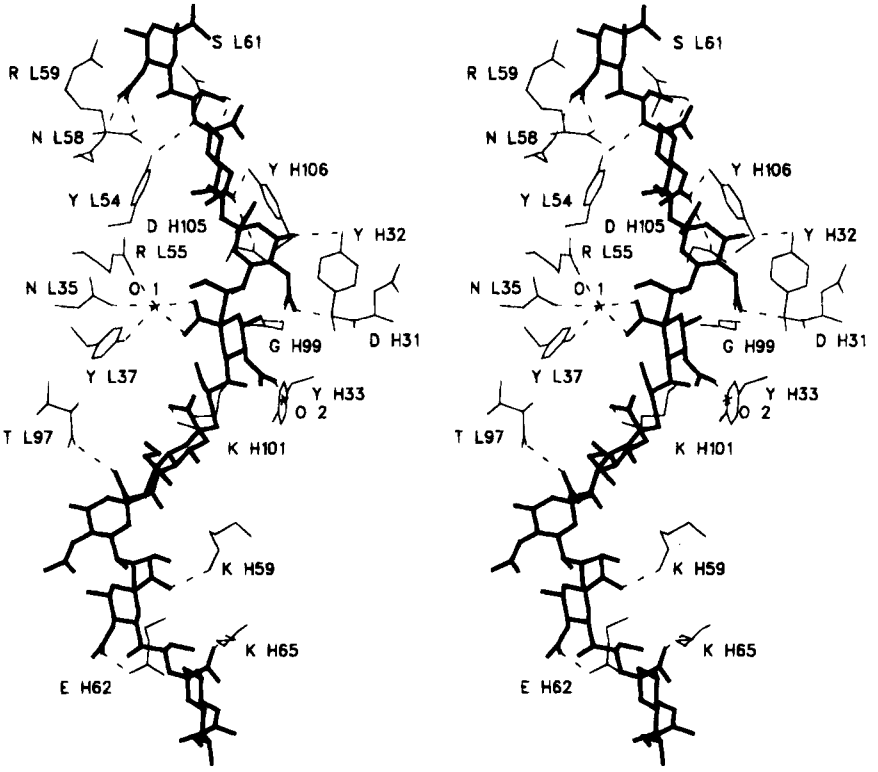

FIGURE 7: Stereoview of the specific contacts made by an eight-residue segment of the oligosaccharide shown in Figure 5a to the surface of the Fab, showing the high degree of complementarily of shape and charge between the protein and carbohydrate. Modeled hydrogen bonds are shown with dashed lines. The protein residues are labeled with their one-letter amino acid code and to indicate their parent light (L) or heavy (H) chain. The oligosaccharide residues run from Sia-2 (top) to Sia-9 (bottom).

The greatest number of interactions between protein and hapten are found along the surface groove on the right side of the Fab as seen in Figure 4 and involving Sia-2−Sia-5. It is in this area that the specificity of mAb735 for *N*-acetyl *vs* *N*-propyl polysialic acid becomes apparent, as a series of hydrogen bonds is formed between several sialic acid residues and the bottom and sides of the groove that would not be possible for the longer *N*-propyl group. One *N*-acetyl group (on Sia-3) forms a hydrogen bond with Asp H105.

Residues Sia-6−Sia-9 are primarily involved through their respective carboxylic acid groups, which take part in one hydrogen bond, and three salt bridges with lysine residues on the protein. There are at least six additional hydrogen bonds that can be readily modeled between the protein and other atoms of the sugar, but the formation of salt bridges between the protein and the carboxylic acid groups of the sialooligosaccharides is an important feature in the recognition of the helix, and compares well with the crystal structure of the complex of a sialic acid analogue with influenza virus neuraminidase (Varghese *et al.*, 1992). It is in this area that the slight cross-reactivity of mAb735 with the *N*-acetyl and *N*-propylneuraminic acid could reside.

Although the charge distribution on the protein is the most significant feature of the left side of Figure 4, a role can also be envisioned for the right side, where the positively-charged Arg L55 is interacting through a bridging water molecule with the carboxylic acid group on Sia-4. The negative charge on Asp H105, located at the bottom of the groove where it can form a hydrogen bond to an *N*-acetyl group, may also serve to direct the orientation of the hapten by repulsing its carboxylic acid groups.

In all, the extended helical model proposed by Brisson *et al.* (1992) with $n = 6$ residues per turn and pitch of $n \times h = 36$ Å has a shape and charge distribution that is complementary to the Fab from mAb735, and can be shown to form a significant number of specific contacts with the Fab over a span at least 8 sialic acid residues in length. This is close to the 10 residues predicted from earlier binding studies (Häyrinen *et al.*, 1989) and is confirmed by our thermodynamic analysis.

CONCLUSIONS

X-ray crystallographic, thermodynamic, and NMR evidence are consistent in the prediction of a binding site on mAb735 which is at least eight residues in length. The crystallographic study is also consistent with the earlier prediction of a helical nature for the antigenic form of the oligosaccharide and provides a molecular basis for the recognition of the *N*-acetylneuraminic acid. Trials are underway to grow crystals of the Fab complexed with oligosaccharides of different lengths; however, no crystals have been obtained to date.

REFERENCES

Baumann, H., Brisson, J.-R., Michon, F., Pon, R., & Jennings, H. J. (1993) *Biochemistry 32*, 4007−4013.

Berg, E. L., Robinson, M. K., Mansson, O., Butcher, E. C., & Magnani, J. L. (1991) *J. Mol. Biol. 266*, 14869−14872.

Brandley, B. K., Swiedler, S. J.,, & Robbins, P. W. (1990) *Cell 63*, 861−863.

Brisson, J.-R., Baumann, H., Imberty, A., Pérez, S., & Jennings, H. J. (1992) *Biochemistry 31*, 4996−5004.

Brünger, A. T. (188) *J. Mol. Biol. 203*, 803−816.

Connolly, M. L. (1981) *Quantum Chem. Program Exchange Bull. 1*, 75.

Corral, L., Singer, M. S., Macher, B. A., & Rosen, S. D. (1990) *Biochem. Biophys. Res. Commun. 172*, 1349−1356.

Cygler, M., Rose, D. R., & Bundle, D. R. (1991) *Science 253*, 442−445.
Evans, S. V. (1993) *J. Mol. Graph. 11*, 134−138.
Finne, J., & Mäkelä, P. H. (1985) *J. Biol. Chem. 260*, 1265−1270.
Fitzgerald, P. M. D. (1988) *J. Appl. Crystallogr. 21*, 273−278.
Frosch, M., Görgen, I., Boulnois, G. J., Timmis, K. N., & Bitter-Suermann, D. (1985) *Proc. Natl. Acad. Sci. U.S.A. 82*, 1194−1198.
Fujinaga, M., & Read, R. (1987) *J. Appl. Crystallogr. 20*, 517−521.
Häyrinen, J., Bitter-Suermann, D., & Finne, J. (1989) *Mol. Immunol. 26*, 523−529.
Jennings, H. J., & Lugowski, C. (1981) *J. Immunol. 127*, 1011−1018.
Jennings, H. J., Katzenellenbogen, E., Lugowski, C., Michon, F., Roy, R., & Kasper, D. L. (1984) *Pure Appl. Chem. 56*, 893−905.
Jennings, H. J., Roy, R., & Michon, F. (1985) *J. Immunol. 134*, 2651−2657.
Kabat, E. A. (1960) *J. Immunol. 84*, 82−85.
Kabat, E. A., Lino, J., Osserman, F., Gamian, A., Michon, F., & Jennings, H. J. (1988) *J. Exp. Med. 168*, 699−711.
Kabat, E. A., Wu, T. T., Perry, H. M., Gottesman, K. S., & Foeller, C. (1991) *Sequences of proteins of immunological interest*, 5th ed., National Institutes of Health, Bethesda, MD.
Klebert, S., Kratzin, H. D., Zimmerman, B., Vaesen, M., Frosch, M., Weisgerber, C., Bitter-Suermann, D., & Hilschmann, N. (1993) *Biol. Chem. Hoppe-Seyler 374*, 993−1000.
Michon, F., Brisson, J.-R., & Jennings, H. J. (1987) *Biochemistry 26*, 8399−8405.
Oomen, R., Young, N. M., & Bundle, D. R. (1991) *Protein Eng. 4*, 427−433.
Phillips, M. L., Nudelmann, E., Gaeta, F. C. A., Perez, M., Singal, A. K., Hakomori, S.-I., & Paulson, J. C. (1990) *Science 250*, 1130−1135.
Ramakrishnan, C., & Ramachandran, G. N. (1965) *Biophys. J. 5*, 909−933.
Rose, D. R., Przybylska, M., To, R. J., Kayden, C. S., Oomen, R. P., Vorberg, E., Young, N. M., & Bundle, D. R. (1993) *Protein Sci. 2*, 1106−1113.
Rutishauser, U., & Jessel, T. M. (1988a) *Phys. Rev. 68*, 819−857.
Rutishauser, U., Acheson, A., Hall, A. K., Mann, D. M., & Sunshine, J. (1988b) Science *240*, 53−57.
Sigurskjold, B. W., Altman, E., & Bundle, D. R. (1991) *Eur. J. Biochem. 197*, 239−246.
Troy, F. A. (1992) *Glycobiology 2*, 5−23.
Vaesen, M., Frosch, M., Weisgerber, C., Eckart, K., Kratzin, H., Bitter-Suermann, D., & Hilschmann, N. (1991) *Biol. Chem. Hoppe*-Seyler *372*, 451−453.
Varghese, J. N., McKimm-Breschkin, J. L., Caldwell, J. B., Kortt, A. A., & Colman, P. M. (1992) *Proteins: Struct., Funct., and Genet. 14*, 327−332.
Vyas, M. N., Vyas, N. K., Meikle, P. J., Sinnott, B., Pinto, B. M., Bundle, D. R., & Quiocho, F. A. (1993) *J. Mol. Biol. 231*, 133−136.
Wessels, M. R., & Kasper, D. L. (1989) *J. Exp. Med. 169*, 2121−2131.
Wessels, M. R., Muñoz, A., & Kasper, D. L. (1987) *Proc. Natl. Acad. Sci. U.S.A. 84*, 9170−9174.
Wiseman, T., Williston, S., Brandts, J. F., & Lin, L.-N. (1989) *Anal. Biochem. 179*, 131−137.
Wyle, F. A., Artenstein, M. S., Brandt, B. L., Tramont, D. L., Kasper, D. L., Altieri, P., Berman, S. L., & Lowenthal, J. P. (1972) *J. Infect. Dis. 126*, 514−522.
Yathindra, N., & Sundaralingam, M. (1976) *Nucleic Acids Res. 3*, 729−747.

BI941119L